ARCHIVES OF MECHANICS
Arch. Mech. **76** (1-2), 191–202, 2024, DOI: 10.24423/aom.4451

Heat conduction in a new Eulerian flow model

M. L. MORRIS

Albuquerque, New Mexico, U.S.A., e-mail: mmorris400@comcast.net

M. Svärd has proposed the Eulerian flow model (EFM) [1] as a replacement for the traditional Navier–Stokes–Fourier (NS) equations. The EFM is equipped with a mass diffusion term in its mass balance law, along with other features, which lead to its satisfying the property of weak well-posedness in the special case of ideal gases with temperature-independent specific heats. Although this property is advantageous mathematically and numerically, it can be shown that the EFM fails to model certain types of problems physically. Here, as an example of the latter, steady-state problems of pure heat conduction are used to show that, when compared with predictions from Fourier's law, the EFM substantially underestimates the magnitude of the heat flux in gases.

Key words: heat conduction in fluids, heat flow measurements, alternative fluid dynamics models, fluid model validation.

1. Introduction

The Navier–Stokes–Fourier (NS) equations can be used to describe a wide variety of fluid behaviors. This system of equations has been in use for almost two centuries and has undergone extensive testing by which its predictions have been compared to measurements of fluid phenomena as diverse as flow through tubes, solid objects falling in fluid media, acoustics, light scattering, and heat transfer, just to mention a few. The NS equations feature three transport coefficients, the shear and bulk viscosities and the thermal conductivity, and although each of these parameters has a molecular dynamical basis in kinetic gas theory, they are interpreted most generally from a phenomenological point of view–that is to say, by measuring their values in gases and liquids in experiments under various thermodynamic conditions. For example, the shear viscosity can be measured by experiments based on Poiseuille flow such as the capillary method (see Bird *et al.* [7, pp. 48–53], for example) the thermal conductivity can be measured with heat transfer experiments such as the hot wire method (see Vargaftik *et al.* [8, pp. 6–8], for example and, assuming the other two parameters are measured independently, the bulk viscosity can be measured by matching ultrasound attenuation data (see Greenspan [9], for example). There are numerous other techniques for measuring the NS transport parameters, but

for a given fluid in a given temperature and pressure state, experiments of high accuracy should all lead to the same values. In practice this is observed, more or less, when the experiments are conducted in the NS range of validity, i.e. not in the highly nonlinear or rarefied gas regimes.

The Eulerian flow model (EFM), proposed by M. Svärd [1] as a replacement for the Navier–Stokes–Fourier equations, is constructed on the idea that transport processes in fluids are governed by one type of diffusion, which leads to a system of equations with a single transport parameter. This simplified view has enabled Svärd to demonstrate weak well-posedness in the special case of an ideal gas with temperature-independent specific heats, and he has exploited this property in computer codes to simulate nonlinear phenomena, such as vortex shedding, with improved numerical behavior when compared to the same type of codes based on the NS equations, which do not satisfy weak well-posedness [1–3].

I believe most researchers would agree that despite any improvements one attempts to make to the NS equations outside their range of validity, it is still necessary to verify that new fluid dynamics models give accurate predictions to problems *within* the NS range of validity. One obvious step towards doing so would be to employ the new formulation in modeling the same type of experiments described above for measuring the NS transport parameters and to compare the results. In Svärd [2] and Dolejší and Svärd [3], the diffusion coefficient in the EFM is chosen effectively to equal the kinematic viscosity, which yields predictions matching those from the NS equations for shear-dominated phenomena like laminar Poiseuille and Couette flow in the continuum regime. I claim that choosing the diffusion coefficient in this manner leads to EFM predictions of both acoustic and thermal phenomena that are highly inaccurate [4–6]. Here, as further support of this claim, I focus on problems of pure steady-state heat conduction to show that the Eulerian flow model greatly underestimates the magnitude of the heat flux in gases.

2. Description of the experiments

The thermal conductivity, λ, in Fourier's law of heat conduction can be measured by experiments like ones described in Vargaftik *et al.* [8, Ch. 2.1] for example, the hot wire method, the concentric cylinders method, and the parallel plates method–whereby a gradient in the temperature, T, is imposed with thermally regulated boundaries across a quiescent fluid. For the types of experiments under discussion, we assume the following.

1. Enough time is allowed to pass so that a steady state in the fluid is reached in which the temperature gradient, ∇T, is constant and the thermodynamic pressure, p, is constant and uniform.

2. Sources of convection have been minimized so that it can be assumed there is no mass flow.
3. The power, Q, to keep the boundaries at their fixed temperatures is measurable, and sources of thermal radiation have been accounted for in the measurement.
4. Conditions of the experiment are chosen to pertain to the continuum regime, where the NS equations are considered to be valid. This means the geometrical length scale, e.g. the characteristic distance between boundaries maintained at different temperatures, is much greater than the characteristic mean free path of the fluid.
5. The temperature difference between thermally regulated boundaries is not extremely large compared to the average temperature so that the experiment does not correspond to the highly nonlinear regime.

In the following section, we study both the NS equations and Svärd's EFM under assumptions 1–3, arriving at the equations to solve for problems in pure steady-state heat conduction. Assumption 4 further allows one to model the fluid as having complete thermal accommodation at thermally regulated boundaries, and assumption 5 ensures that one may approximate the transport parameters as being constant on the domain. In Appendix A, we use the parallel plates method to illustrate these general concepts with a simple example.

3. Mathematical models

3.1. Navier–Stokes Model

Throughout this discussion, standard tensor operators have been employed, see BIRD *et al.* [7] for example, and the symbol, I, is used to denote the second-order identity tensor. The NS equations can be expressed as the following system:

$$\frac{\partial \rho}{\partial t} = -\nabla \cdot (\rho \mathbf{v}), \tag{3.1}$$

$$\frac{\partial (\rho \mathbf{v})}{\partial t} = -\nabla \cdot (p\mathsf{I} - \Pi_v + \rho \mathbf{v}\mathbf{v}), \tag{3.2}$$

and

$$\frac{\partial E}{\partial t} = -\nabla \cdot (\mathbf{q} - \Pi_v \cdot \mathbf{v} + (E + p)\mathbf{v}). \tag{3.3}$$

In the above, ρ represents the mass density, $\mathbf{v}$ denotes the velocity vector, and E is the total energy density, which is the sum of the internal energy density and

the kinetic energy density:

$$E = \rho u + \frac{1}{2}\rho \mathbf{v}\cdot\mathbf{v}, \tag{3.4}$$

where the specific internal energy is denoted as u. The viscous stress tensor is taken to be that of a Newtonian fluid:

$$\Pi_v = \zeta(\nabla\cdot\mathbf{v})\mathsf{I} + 2\eta\nabla\mathbf{v}^{SD}, \tag{3.5}$$

where ζ and η are the bulk and shear viscosity, respectively, and "SD" is used to denote the symmetric and deviatoric part of a tensor; and the heat flux is given by Fourier's law:

$$\mathbf{q} = -\lambda\nabla T, \tag{3.6}$$

where λ represents the thermal conductivity.

Let us study a fluid on a fixed spatial domain Ω with closed boundary, $\partial\Omega$. Integrating (3.1)–(3.3) over the volume Ω, applying Gauss's divergence theorem, and assuming there to be no total change in mass or momentum, leads to

$$0 = \int_\Omega \frac{\partial\rho}{\partial t}\,dV = -\oint_{\partial\Omega} \mathbf{n}\cdot(\rho\mathbf{v})\,dA, \tag{3.7}$$

$$\mathbf{0} = \int_\Omega \frac{\partial(\rho\mathbf{v})}{\partial t}\,dV = -\oint_{\partial\Omega} \mathbf{n}\cdot(p\mathsf{I} - \Pi_v + \rho\mathbf{v}\mathbf{v})\,dA, \tag{3.8}$$

and

$$-Q = \int_\Omega \frac{\partial E}{\partial t}\,dV = -\oint_{\partial\Omega} \mathbf{n}\cdot(\mathbf{q} - \Pi_v\cdot\mathbf{v} + (E+p)\mathbf{v})\,dA, \tag{3.9}$$

where, we recall from Section 2 that Q represents the total power required to maintain the thermally regulated boundaries and, under assumptions 1 and 3, this is a constant measurable quantity.

Also recall that we suppose there to be no mass flux under assumption 2, which means $\rho\mathbf{v}$–and, thereby, $\mathbf{v}$–are zero. Therefore, the above system reduces to

$$\oint_{\partial\Omega} p\mathbf{n}\,dA = \mathbf{0},$$

a condition that is automatically satisfied under assumption 1, and

$$-\oint_{\partial\Omega} \mathbf{n}\cdot\mathbf{q}\,dA = \oint_{\partial\Omega} \mathbf{n}\cdot(\lambda\nabla T)\,dA = -Q. \tag{3.10}$$

Using Gauss's divergence theorem again, we see that in order to find the temperature profile, one must solve

$$\int_{\Omega} \nabla \cdot (\lambda \nabla T)\, dV = -Q. \tag{3.11}$$

The above relationship is routinely used to measure values for the thermal conductivity, λ, of fluids–for example, see Appendix A for a discussion of how this is done with the parallel plates method. Therefore, $\mathbf{q}$ given by Fourier's law represents the heat flux that is physically measured in pure heat conduction experiments.

3.2. The Eulerian Flow Model proposed by SVÄRD [1, 2]

The EFM proposed in SVÄRD [1, Eqs. (34)] is the following system of balance laws for the mass, momentum, and total energy:

$$\frac{\partial \rho}{\partial t} = -\nabla \cdot (-\nu \nabla \rho + \rho \mathbf{v}), \tag{3.12}$$

$$\frac{\partial (\rho \mathbf{v})}{\partial t} = -\nabla \cdot (p\mathsf{I} - \nu \nabla (\rho \mathbf{v}) + \rho \mathbf{v}\mathbf{v}), \tag{3.13}$$

and

$$\frac{\partial E}{\partial t} = -\nabla \cdot (-\nu \nabla E + (E + p)\mathbf{v}), \tag{3.14}$$

where ν is a diffusion parameter, chosen in SVÄRD [2] and DOLEJŠÍ and SVÄRD [3], effectively to equal to the kinematic viscosity,

$$\nu = \frac{\eta}{\rho}, \tag{3.15}$$

in order to make predictions that agree well with those from the NS equations for shear-dominated phenomena.

Our next goal is to determine the purely conductive heat flux in the EFM for comparison with Fourier's law (3.6) in the NS model. If, as before, one integrates (3.12)–(3.14) over the domain Ω, and assumes there to be no total change in mass or momentum, then one obtains:

$$0 = \int_{\Omega} \frac{\partial \rho}{\partial t}\, dV = -\oint_{\partial \Omega} \mathbf{n} \cdot (-\nu \nabla \rho + \rho \mathbf{v})\, dA, \tag{3.16}$$

$$\mathbf{0} = \int_{\Omega} \frac{\partial (\rho \mathbf{v})}{\partial t}\, dV = -\oint_{\partial \Omega} \mathbf{n} \cdot (p\mathsf{I} - \nu \nabla (\rho \mathbf{v}) + \rho \mathbf{v}\mathbf{v})\, dA, \tag{3.17}$$

and

$$-Q = \int_{\Omega} \frac{\partial E}{\partial t}\, dV = -\oint_{\partial\Omega} \mathbf{n} \cdot (-\nu \nabla E + (E+p)\mathbf{v})\, dA. \tag{3.18}$$

The total mass flux in the EFM is given by $-\nu\nabla\rho + \rho\mathbf{v}$, and its terms must balance as

$$\nu \nabla \rho = \rho \mathbf{v} \tag{3.19}$$

in order for the fluid to exhibit no mass flow per assumption 2. Next, if one uses tensor identity (B.1) and takes p to be uniform by assumption 1, the steady-state momentum equation (3.17) becomes

$$\oint_{\partial\Omega} \mathbf{n} \cdot (\nu\rho\nabla\mathbf{v} + \nu(\nabla\rho)\mathbf{v} - \rho\mathbf{v}\mathbf{v})\, dA = \mathbf{0}$$

or, enforcing the no-mass-flow condition (3.19),

$$\oint_{\partial\Omega} \mathbf{n} \cdot (\nu\rho\nabla\mathbf{v})\, dA = \mathbf{0}. \tag{3.20}$$

Let us now examine the steady-state total energy equation (3.18). Substituting definition (3.4) yields

$$-\oint_{\partial\Omega} \mathbf{n} \cdot \left(-\nu\nabla(\rho u) - \frac{\nu}{2}\nabla(\rho\mathbf{v}\cdot\mathbf{v}) + (\rho u + p + \frac{1}{2}\rho\mathbf{v}\cdot\mathbf{v})\mathbf{v}\right) dA = -Q \tag{3.21}$$

which, upon use of tensor identities (B.2) and (B.3), becomes

$$-\oint_{\partial\Omega} \mathbf{n} \cdot \begin{pmatrix} -\nu\rho\nabla u - u\nu\nabla\rho - \frac{\nu}{2}(\nabla\rho)\,\mathbf{v}\cdot\mathbf{v} + \\ -\nu\rho\,(\nabla\mathbf{v})\cdot\mathbf{v} + \left(\rho u + p + \frac{1}{2}\rho\mathbf{v}\cdot\mathbf{v}\right)\mathbf{v} \end{pmatrix} dA = -Q. \tag{3.22}$$

As computation 1 in Appendix B, it is shown that condition (3.20) leads to

$$\oint_{\partial\Omega} \mathbf{n} \cdot (\nu\rho(\nabla\mathbf{v})\cdot\mathbf{v})\, dA = 0, \tag{3.23}$$

and by using this and relation (3.19) in the above, one arrives at

$$-\oint_{\partial\Omega} \mathbf{n} \cdot \left(-\nu\rho\nabla u + \frac{p}{\rho}\nu\nabla\rho\right) dA = -Q. \tag{3.24}$$

Finally, substitution of the thermodynamic relationships (B.5) and (B.6), under assumption 1 that p is uniform, yields

$$\oint_{\partial\Omega} \mathbf{n} \cdot (\nu\rho c_P \nabla T)\, dA = -Q. \tag{3.25}$$

Comparing this with (3.10) and using (3.15), one finds the heat flux for pure steady-state heat conduction in the EFM is given by

$$\mathbf{q}_{EFM} = -\eta c_P \nabla T. \tag{3.26}$$

4. Comparison of model predictions to experiments

Recall that $\mathbf{q}$, given by Fourier's law (3.6) with recorded values of λ, represents the physical heat flux that is measured in the experiments under discussion. Taking the ratio of the magnitudes of the NS and EFM heat fluxes, one finds

$$\frac{|\mathbf{q}_{EFM}|}{|\mathbf{q}|} = \frac{\eta c_P}{\lambda} = \mathrm{Pr}, \tag{4.1}$$

where Pr is the Prandtl number. A table containing values of the Prandtl number for a few different fluids at room temperature (in the range 293–300 K) is provided below.

Fluid	Pr
noble gas	0.667
hydrogen gas	0.690
nitrogen gas	0.719
oxygen gas	0.727
methane gas	0.728
carbon dioxide gas	0.763
water	6.9

As the table demonstrates, ideal gases typically have measured Prandtl numbers near the value of 0.7, which in view of equation (4.1) implies that the EFM systematically underestimates heat flow in this type of medium. On the other hand, water and other liquids typically have Prandtl numbers much higher than 1, resulting in greatly overestimated EFM heat flow predictions.

5. Discussion

From the present results and the results contained in [4–6], I contend that although it exhibits the desired property of weak well-posedness in ideal gases with

temperature-independent specific heats, Svärd's Eulerian flow model is based on an oversimplified view of diffusion processes in fluids–one that leads to inaccurate predictions for both thermal and acoustic phenomena in the NS range of validity. I argue, therefore, that Svärd's model is not a viable replacement for the Navier–Stokes–Fourier equations. Moreover, it is seen that by comparing only numerical results from different fluid dynamics models – without attempting to relate the models to a wide variety of physical experiments in which data is available – one runs the risk of favoring a simpler set of equations that might be numerically better-behaved in the type of code for which it has been tailored, but that ultimately describes nature less accurately.

Appendix A. Parallel plates method

Let us consider a laboratory experiment that may be used to measure the thermal conductivity λ, of a fluid. The following parallel plates method is described in more detail in Vargaftik *et al.* [8, Ch. 2.1] and Teagan and Springer [10], where there appear discussions of how to account for and/or eliminate potential sources of error, e.g. those that might arise from thermal convection and radiation[1]. Its simple one-dimensional Cartesian geometry is my reason for choosing to provide it as an example for pure heat conduction.

Suppose there is an unperturbed fluid at pressure p between two parallel plates, each having an area A and set a distance L apart. Each plate is maintained at a different temperature, the colder plate at T_c and the hotter one at T_h. After a steady state has been reached, a measurement is made of the power, Q, required to keep the plates at their respective temperatures. For example, in Teagan and Springer's experiment from [10], Q is measured as the total electrical power input of the hot plate heating element minus the power loss measured from experiments conducted in a vacuum, which accounts for thermal radiation effects. Additional specifications regarding the parallel plates method for measuring λ are listed below.

1. The plates are oriented perpendicular to the direction of gravity, with the hotter plate above the colder plate so as to minimize convective effects.
2. The plates are maintained at uniform temperatures across their surfaces with their diameters much larger than the spacing, L, between them so that the experiment can be modeled as approximately one-dimensional.
3. The temperature difference between the plates, $\Delta T = T_h - T_c$, is not large compared to the average temperature, $T_0 = (T_h + T_c)/2$. This ensures the

[1]Note, however, that Teagan and Springer in [10] use their apparatus to study gases in the transition regime, whereas here our focus is on gases in the continuum regime.

experiment does not correspond to the highly nonlinear regime and one can model the transport coefficients like the thermal conductivity λ, as being approximately constant throughout the domain.

4. L is much greater than the characteristic mean free path length of the fluid, which for an ideal gas is of the order, $\eta\sqrt{\mathcal{R}T_0}/p$, where $\mathcal{R}$ is the specific gas constant. This ensures the experiment belongs to the continuum regime and it is appropriate to model the fluid as having complete thermal accommodation with the plates, i.e. to assume the fluid's temperature is equal to that of the plates at the boundaries.

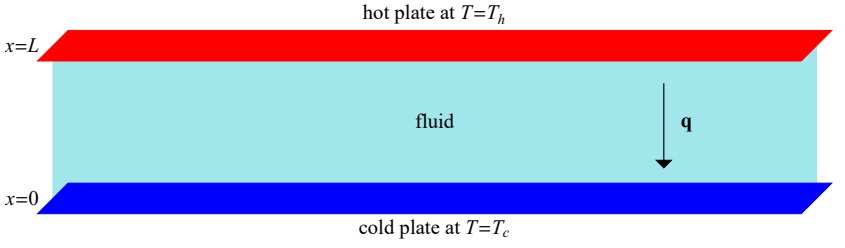

FIG. 1. Parallel plates method.

As shown in Fig. 1, let us suppose that the spatial variation occurs in the Cartesian x-variable and that the cold and hot plates are located at $x = 0$ and $x = L$, respectively. In Section 3.1, we find that the heat conduction experiment described above is modeled in the NS formulation by (3.11), which for our one-dimensional problem, under assumptions 3 and 4 above, becomes

$$\int \left(\lambda \frac{d^2T}{dx^2}\right) dx = \frac{Q}{A} \tag{A.1}$$

with boundary conditions,

$$T(0) = T_c \quad \text{and} \quad T(L) = T_h. \tag{A.2}$$

Therefore, the temperature is found by solving

$$\frac{dT}{dx} = \frac{Q}{A\lambda} \tag{A.3}$$

with (A.2), which yields the linear profile:

$$T(x) = T_h + \frac{\Delta T}{L}(x - L). \tag{A.4}$$

Substituting the temperature gradient computed from (A.4) into (A.3), one finds the thermal conductivity is given by

$$\lambda = \frac{QL}{A\Delta T}, \tag{A.5}$$

where each of the quantities on the right-hand side is measurable in the experiment.

Appendix B. Formulas and computations

Tensor identities. In Section 3.2 and below, we use the following tensor identities:

$$\nabla(\alpha\mathbf{w}) = \alpha\nabla\mathbf{w} + (\nabla\alpha)\mathbf{w}, \tag{B.1}$$

$$\nabla(\alpha\beta) = \alpha\nabla\beta + \beta\nabla\alpha, \tag{B.2}$$

$$\nabla(\mathbf{w}\cdot\mathbf{w}) = 2(\nabla\mathbf{w})\cdot\mathbf{w} \tag{B.3}$$

and

$$\nabla\cdot(\mathsf{M}\cdot\mathbf{w}) = \mathsf{M}^T\colon\nabla\mathbf{w} + (\nabla\cdot\mathsf{M})\cdot\mathbf{w}, \tag{B.4}$$

where α and β represent scalar functions, $\mathbf{w}$ is a vector function, and M is a second-order tensor function with transpose denoted as M^T. The double-dot operator " : " in Eq. (B.4) represents the inner tensor product.

Thermodynamic relationships. In Section 3.2, we employ the following equilibrium thermodynamic relationships:

$$d\rho = -\rho\alpha_P dT + \frac{\gamma}{c^2}dp \tag{B.5}$$

and

$$du = \left(c_P - \frac{p\alpha_P}{\rho}\right)dT + \frac{1}{\rho}\left(\frac{\gamma p}{\rho c^2} - T\alpha_P\right)dp, \tag{B.6}$$

where ρ is mass density, u is specific internal energy, T is absolute temperature, p is thermodynamic pressure, α_P is the thermal expansion coefficient, c_P is the isobaric specific heat, $\gamma = c_P/c_V$ is the ratio of isobaric to isochoric specific heat, and c is the adiabatic sound speed. The above relationships can be derived using techniques presented in [11, Ch. 5], for example.

Additional computations

1. Using Gauss's divergence theorem, tensor identity (B.4), and condition (3.20), one computes

$$\begin{aligned}(\text{B.7}) \qquad \oint_{\partial\Omega} \mathbf{n}\cdot(\nu\rho(\nabla\mathbf{v})\cdot\mathbf{v})\,dA &= \int_{\Omega} \nabla\cdot(\nu\rho(\nabla\mathbf{v})\cdot\mathbf{v})\,dV \\ &= \int_{\Omega} (\nabla\cdot(\nu\rho\nabla\mathbf{v})\cdot\mathbf{v} + \nu\rho\nabla\mathbf{v}^T\colon\nabla\mathbf{v})\,dV \\ &= \oint_{\partial\Omega} \mathbf{n}\cdot(\nu\rho\nabla\mathbf{v})\cdot\mathbf{v}\,dA + \int_{\Omega} \nu\rho\nabla\mathbf{v}^T\colon\nabla\mathbf{v}\,dV \\ &= \int_{\Omega} \nu\rho\nabla\mathbf{v}^T\colon\nabla\mathbf{v}\,dV\,dV.\end{aligned}$$

The integrand in the final line on the right-hand-side of (B.7), is the viscous dissipation in Svärd's EFM, and for problems in pure heat conduction, it is reasonable to assume this quantity is negligible, in which case the above implies (3.23):

$$\oint_{\partial\Omega} \mathbf{n}\cdot(\nu\rho(\nabla\mathbf{v})\cdot\mathbf{v})\,dA = 0.$$

2. In [12, Eqs. (2)] and later in a section titled "Tentative update of the modified model", Svärd and Munthe discuss the idea of changing the original EFM from [1] by replacing the energy balance equation (3.14) with the following:

$$\frac{\partial E}{\partial t} = \nabla\cdot(\nu\nabla E - (E+p)\mathbf{v} + \kappa\nabla T). \tag{B.8}$$

The authors do not investigate thermal phenomena in [12]. However, using similar analysis as in Section 3.2, I compute the altered EFM heat flux for pure steady-state heat conduction as

$$\mathbf{q}_{EFM} = -(\eta c_P + \kappa)\nabla T. \tag{B.9}$$

To match heat conduction experiments with the above, one would enforce $\mathbf{q}_{EFM} = \mathbf{q}$, and doing so, I find

$$\kappa = \eta c_P\left(\frac{1}{\mathrm{Pr}} - 1\right). \tag{B.10}$$

In my earlier study [6, Eq. (35)], I observed this parameter must be chosen as

$$\kappa = \eta c_P\left(\frac{1}{\mathrm{Pr}} + \frac{1}{\gamma-1}\left(\frac{\zeta}{\eta} - \frac{2}{3}\right)\right) \tag{B.11}$$

in order to match sound attenuation experiments. If one takes

$$\zeta = 0 \quad \text{and} \quad \gamma = 5/3$$

in the special case of ideal noble gases, then the value for κ computed by the two formulas in (B.10) and (B.11) match. However, in general, these equations give significantly different values for κ.

Acknowledgements

I am very grateful to my father, Dr. Marvin Morris, for obtaining for me many of the references in my bibliography, to Frances Grishkina-Santangelo for generating the figure appearing in Appendix A, and to Prof. Jacek Pozorski of Institute of Fluid-Flow Machinery, Polish Academy of Sciences, for reading earlier drafts of this article and providing helpful suggestions and encouragement.

References

1. M. Svärd, *A new Eulerian model for viscous and heat conducting compressible flows*, Physica A, **506**, 350–375, 2018.
2. M. Svärd, *Analysis of an alternative Navier-Stokes system: weak entropy solutions and a convergent numerical scheme*, technical report, 2021, ResearchGate, preprint, doi: 10.13140/RG.2.2.16184.47366.
3. V. Dolejší, M. Svärd, *Numerical study of two models for viscous compressible fluid flows*, Journal of Computational Physics, **427**, 110068, 2021.
4. M. Morris, *Analysis of an alternative Navier-Stokes system: attenuation of sound waves*, ResearchGate preprint, doi: 10.13140/RG.2.2.29383.01442, 2021.
5. M. Morris, *Analysis of an alternative Navier–Stokes system: Rayleigh–Brillouin light scattering*, ResearchGate preprint, doi: 10.13140/RG.2.2.32239.92321, 2022.
6. M. Morris, *Sound Attenuation in the Modified Navier–Stokes Equations of Svärd*, doi: 10.13140/RG.2.2.11772.92809, 2023.
7. R.B. Bird, W.E. Stewart, E.N. Lightfoot, *Transport Phenomena*, 2nd ed., John Wiley & Sons, Inc., New York, 2002.
8. N.B. Vargaftik, *Handbook of Thermal Conductivity of Liquids and Gases*, 1st ed., CRC Press, Boca Raton, 1993.
9. M. Greenspan, *Rotational relaxation in nitrogen, oxygen, and air*, Journal of the Acoustical Society of America, **31**, 2, 155–160, 1959.
10. W.P. Teagan, G.S. Springer, *Heat-transfer and density-distribution measurements between parallel plates in the transition regime*, The Physics of Fluids, **11**, 3, 497–506, 1968.
11. H.B. Callen, *Thermodynamics*, John Wiley & Sons, New York, London, 1962.
12. M. Svärd, K. Munthe, *A study of the diffusive properties of a modified compressible Navier–Stokes model*, Meccanica, **58**, 1083–1097, 2023.

Received November 22, 2023; revised version February 17, 2024.
Published online February 29, 2024.